ACS APPLIED MATERIALS & INTERFACES

Research Article

www.acsami.org

Terms of Use

Combinatorial Discovery Through a Distributed Outreach Program: Investigation of the Photoelectrolysis Activity of p-Type Fe, Cr, Al Oxides

John G. Rowley,[†] Thanh D. Do,[§] David A. Cleary,[‡] and B. A. Parkinson*

Department of Chemistry and School of Energy Resources, University of Wyoming, Laramie, Wyoming 82071, United States

Supporting Information

ABSTRACT: We report the identification of a semiconducting p-type oxide containing iron, aluminum, and chromium ($Fe_{2-x-y}Cr_xAl_yO_3$) with previously unreported photoelectrolysis activity that was discovered by an undergraduate scientist participating in the Solar Hydrogen Activity research Kit (SHArK) program. The SHArK program is a distributed combinatorial science outreach program designed to provide a simple and inexpensive way for high school and undergraduate students to participate in the search for metal oxide materials that are active for the photoelectrolysis of water. The identified $Fe_{2-x-y}Cr_xAl_yO_3$ photoelectrolysis material possesses many properties that make it a promising candidate for further optimization for potential application in a photoelectrolysis device. In addition to being composed of earth abundant elements, the FeCrAl oxide material has a band gap of 1.8 eV. Current−potential measurements for $Fe_{2-x-y}Cr_xAl_yO_3$ showed an open circuit photovoltage of nearly 1 V; however, the absorbed photon conversion efficiency for hydrogen evolution was low (2.4×10^{-4} at 530 nm) albeit without any deposited hydrogen evolution catalyst. X-ray diffraction of the pyrolyzed polycrystalline thin $Fe_{2-x-y}Cr_xAl_yO_3$ film on fluorine-doped tin oxide substrates shows a hexagonal phase (hematite structure) and scanning electron microscope images show morphology consisting of small crystallites.

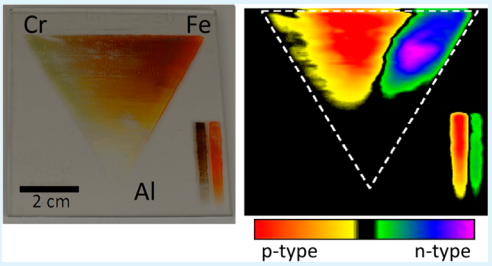

KEYWORDS: *combinatorial chemistry, undergraduate research, distributed research program, photoelectrochemical activity, metal oxide photocatalyst, solar hydrogen research*

INTRODUCTION

Solar energy is the most abundant renewable energy source available in our terrestrial environment[1] but the inability to efficiently and inexpensively store it may present the largest obstacle for a transition to a solar powered economy.[2] Water electrolysis, to produce hydrogen fuel, is a promising strategy for storing solar energy. Conventional photovoltaic cells connected to commercial electrolyzers could already be used to store solar energy; however, these technologies may prove cost prohibitive. Direct photoelectrolysis of water using an immersed metal oxide semiconductor photoelectrode could be an inexpensive method to convert solar energy to storable hydrogen fuel if it could be accomplished efficiently with inexpensive thin film photelectrodes. Metal oxides can be inexpensive, thermodynamically stable, absorb visible light, and can be stable to chemical decomposition under photoelectrolysis conditions, making them ideal candidate materials for photelectrolysis electrodes.[3] Unfortunately, there are still no known semiconducting metal oxide materials that have the proper set of characteristics for efficient water photoelectrolysis making the discovery of such materials a priority for the scientific community where large research centers have been established to conduct fundamental research and develop an operational photoelectrolysis device.[4] Discovery of suitable material compositions is only the first step on the path to fabricating a useful metal oxide photoelectrolysis device, the subsequent steps of material optimization, material nanostructuring, catalyst optimization, membrane optimization, and device prototyping all must be completed before a functioning device is implemented.

The yet undiscovered photoelectrolysis metal oxide materials will most likely be a complex combination of three or more elements due to the many requirements of their physical and chemical properties.[3] It is currently not possible to *a priori* calculate the structure and atomic composition of candidate metal oxide photoelectrolysis materials; therefore, a multitude of multicomponent metal oxide combinations must be synthesized and screened. Given that there are ∼50 possible candidate metals, this would be approximately 19,000 combinations for the ternary oxides and 220,000 combinations for quaternary metal oxides if the stoichiometric ratios were constrained to be 1:1:1 and substantially higher with the many possible stoichiometries. Therefore, we developed a combinatorial method using ink jet printing of metal oxide precursors to facilitate the discovery process.[3]

Received: December 31, 2013
Accepted: March 26, 2014
Published: March 26, 2014

 © 2014 American Chemical Society dx.doi.org/10.1021/am406045j | ACS Appl. Mater. Interfaces 2014, 6, 9046−9052

To accelerate the discovery of new metal oxide semiconductors that exhibit photoelectrolysis activity, and realizing the large number of possible materials to screen in our research program, the Solar Hydrogen research Activity Kit (SHArK) project was established in 2008. The SHArK project enlists high school and undergraduate students to help sort through the many possible metal oxide compositions to identify new photoelectrolysis materials.[5] The SHArK distributed research program provided the students with the materials that they needed, including an inexpensive laser-rastering apparatus based on a LEGO Mindstorm kit, an electrochemical cell, an electronics box for data collection, and FTO plates. The students prepared multi-element metal oxide thin films by spraying, pipetting drops of premixed precursors or ink jet printing metal nitrate salt precursors onto the FTO substrate, and pyrolyzing the sample to form mixed metal oxides. The metal oxide thin films are then immersed in aqueous electrolyte and the SHArK kit laser scanner, which uses an inexpensive green laser pointer, was used to interrogate the multi-element metal oxide thin film for regions of visible light initiated photoelectrolysis activity. To date, over 70 SHArK kits have been provided to young scientists. The curiosity, creativity, and persistence of these young scientists resulted in the fabrication and screening of hundreds of multi-metal oxide materials using a variety of methods. In 2009, undergraduate researchers at Gonzaga University, participating in the SHArK program using an off-the-shelf Hewlett Packard ink jet printer, discovered and reported on the SHArK Web site (www.thesharkproject.org) a potentially promising ternary photoelectrolysis material containing a combination of iron, chromium, aluminum, and cesium (Figure S1, Supporting Information).[9,10] The participating undergraduates and high school students usually do not have the facilities to characterize the composition and structure of the materials they have identified, and so herein we report a more detailed investigation of a semiconducting p-type FeCrAl oxide material with previously unreported photoelectrolysis properties.

EXPERIMENTAL SECTION

Printing of Electrodes. $Fe(NO_3)_3$ (Fisher Scientific), $Cu(NO_3)_2$ (Sigma-Aldrich), $Cr(NO_3)_3$ (Alfa Aesar), and $Al(NO_3)_3$ (Fisher Scientific) were used as received. Diethylene glycol (Sigma-Aldrich) and diethylene glycol monobutyl ether (Fluka) were used as received. Fluorine-doped tin oxide (FTO) substrates were obtained from Hartford Glass Inc. The FTO substrates were hand washed with Aquanox and a copious rinsing with 18 MΩ H_2O and methanol before use. Ink solutions were prepared by dissolving 0.5 M metal nitrate salts in an ink base that was an aqueous solution of 35% diethylene glycol and 1% diethylene glycol monobutyl ether by volume. The solutions were sonicated and filtered through a 2 μm syringe filter into empty ink cartridges.

An inkjet printing technique described previously was used to deposit the metal nitrate salt precursors onto the FTO substrates.[6,7] Briefly, a Fujifilm Dimatix piezoelectric ink jet printer was used to deposit thin films ink solutions of 0.5 M nitrate metal salt onto the FTO substrate by repeated precision jetting of 7 pL drops with a spacing between drops of 20−30 μm. Optimal piezoelectric ink jet nozzle performance was achieved by running multiple cleaning cycles and confirmed using the printer head camera. As discussed previously, the piezoelectric jetting waveform, frequency of nozzle firing, substrate temperature, and ink composition can all be important parameters for printing high quality metal oxide thin films.

Homogenous mixing of the printed metal nitrate salt precursors on the sub-millimeter scale is desirable, whereas mixing on the centimeter scale is undesirable when printing gradient patterns. Mixing on the sub-millimeter scale was promoted by choosing a drop spacing where the approximately hemispherical 7 pL droplets on the FTO substrate would just overlap and coalesce. A hemispherical approximation of the 7 pL drop volume yields an ∼30 μm diameter spot, thus drop spacings substantially greater than 30 μm were avoided. Maintenance of the piezoelectric ink jet printer heads incorporated into each ink cartridge was key to generating high quality metal oxide thin films. After each use, the ink jet printer head was disconnected from the ink cartridge and gently flushed with 18 MΩ H_2O to remove any residual salts or glycols from the nozzles. The ink jet printer heads were allowed to dry between experiments and were stored detached from the ink cartridge. The metal nitrate salts deposited onto the FTO substrate were pyrolyzed in air with an 11 °C/min heating ramp rate to a 525 °C dwell temperature for 1.5 h using a Lindberg Blue M furnace to produce the metal oxide thin film.

Printing templates were designed using Adobe Photoshop 7.0 software. Both discrete patterns and gradient patterns were employed. Calibration curves were developed to correlate the pixel density within the Photoshop image to the actual drop density deposited onto the FTO substrate in the printing process.

Photocurrent Mapping. False color photocurrent images for the metal oxide thin films on FTO substrates were measured using a procedure described previously.[6,7] Briefly, the photocurrent produced by rastering a laser beam over the metal oxide thin film while in an electrolyte was used to generate a false color image to show regions of photoelectrolysis activity. A schematic of the scanning laser system is shown in Figure S2 (Supporting Information). False color photocurrent images were measured by immersing the metal oxide thin film on the FTO substrate into a 0.1 M NaOH aqueous electrolyte. The FTO substrate was connected as the working electrode to a Princeton Applied Research 174A potentiostat in an electrochemical cell with a 9 × 9 cm carbon plate acting as both the counter and reference electrode in a two electrode configuration. The metal oxide thin film was irradiated with a 532 nm laser with a beam full width at half max of approximately 1 mm and an intensity of less than 20 mW. The laser beam was modulated with a chopper (Photon Technology International OC-4000) operating at 27 Hz and was rastered over the metal oxide thin film with the aid of two galvanometer mirrors (Eye Magic EMS-4000 infinity). A lock-in amplifier (Stanford Research 530) was used to phase detect the photocurrent that was recorded for each location on the metal oxide thin film sample and assigned as the z value on the corresponding $x-y$ pixel location of the false color photocurrent maps. The electrolyte was not purged of oxygen during initial false color photocurrent imaging because the photocurrent mapping experiment is designed for rapid screening of photoactive semiconductor candidates; therefore, some of the photocurrent generated by p-type materials could be due oxygen reduction.

A unique aspect of acquiring false color photocurrent images is that the effective working electrode (the laser illuminated current generating region) changes position by up to 8 cm during the experiment as the laser rasters across the metal oxide thin film. If a two-electrode configuration is used and the reference/counter electrode is relatively small, the solution resistance will change with the position of the laser spot. This resistance drop change will influence the false color photocurrent image. Therefore, a carbon plate the same size as the working electrode (9 × 9 cm) was used as a counter/reference and the working and counter/reference electrodes were held parallel to each other at a separation distance of 2 cm. The carbon plate was also an effective beam stop that prevented unwanted laser reflections.

Incident Photon Conversion Efficiency Spectra. The incident photon to current efficiency (IPCE) spectra of the metal oxide thin films were acquired in aqueous 0.1 M perchloric acid solution. The electrolyte solution was de-oxygenated under an argon stream then continuously purged with $H_2(g)$ during the measurement. The metal oxide thin film printed onto a FTO substrate was connected to a potentiostat as the working electrode (Princeton Applied Research 174A) in a three electrode configuration with an Ag/AgCl reference electrode and a platinum wire counter electrode. The metal oxide thin film electrode was illuminated with a 50 W tungsten lamp that was

wavelength selected through a custom software program that controlled a motorized monochromoter (Jobin Yvon Model H-20) and recorded photocurrent values at each excitation wavelength to generate the IPCE spectra. The excitation beam was modulated with a chopper (Stanford Research Systems Model 540) operating at 27 Hz and passed through the FTO before illuminating the metal oxide film (back-side illumination). The lock-in amplified (Stanford Research Systems Model SR830 DSP) current was read for each wavelength to generate a spectrum using a custom computer program.

Current−Potential Curves. Current−Potential (IV) curves for the metal oxide thin films were acquired in aqueous 0.1 M perchloric acid solution. The electrolyte solution was de-oxygenated under an argon stream and then continuously purged with $H_2(g)$ during the measurement.[8] An Ivium potentiostat in a three electrode configuration was used to measure the current−potential response of the metal oxide thin film working electrode on a FTO substrate. The reference electrode was Ag/AgCl and the counter electrode was a platinum (Pt) wire. All IV measurements were done vs a Ag/AgCl electrode and adjusted to the thermodynamic reversible hydrogen electrode (RHE) potential in this electrolyte. The thermodynamic potential for proton reduction in this electrolyte is calculated to be at −0.258 V vs the Ag/AgCl electrode and was measured on clean platinum electrode to be approximately at that value. The approximate 200 nm thick FeAlCr oxide thin film electrode was illuminated with an expanded 532 nm laser beam with a power of 100 mW, irradiating an area of 1.76 cm^2. The illuminating laser light passed through the FTO before impinging on the metal oxide film (back-side illumination). The sweep rate was 0.01 V/s.

X-ray Diffraction of Metal Oxide Thin Films. Glancing angle thin film X-ray diffraction (XRD) patterns were measured using a Rigaku XRD SmartLab X-ray Diffractometer using Cu Kα radiation. Diffraction patterns were acquired on large area pyrolyzed metal oxide thin films that were approximately 200 nm thick on a FTO substrate printed using an identical protocol as the for photoelectrolysis samples. The XRD patterns were acquired at a glancing ω angle of 0.5° and a 2θ step size of 0.05°. Even at such an acute ω angle, X-ray scattering peaks from the underlying FTO substrate are present in all the metal oxide thin film diffraction patterns. Lattice parameters were calculated from the XRD patterns using PDLX Rigaku data analysis software.

Scanning Electron Microscope Imaging. Backscattered electron images were measured using a FEI Quanta FEG 450 field emission scanning electron microscope (FE-SEM) at a vacuum >1 × 10^{-5} Torr.

RESULTS AND DISCUSSION

The p-type photoelectrolysis activity of a ternary metal oxide resulting from mixing iron, chromium, and aluminum precursors reported on the SHArK website was confirmed by printing these metals in a triangular gradient pattern that we have used previously.[6,7] Figure 1a shows a p-type photoactive region between the iron and chromium vertices that extends out towards the aluminum vertex that exceeds the photoresponse of the p-type internal standard copper oxide. Although it is tempting to assign the photocatalytic activity of a location to a phase containing the relative metal stoichiometry estimated from the printed stoichiometry, the identity of the photoactive phase depends on the thermodynamics of the phase stability (the phase diagram), the solubility of each element in the various phases and the mechanism and kinetics of the phase formation because amorphous phases may also be present. Indeed, the photoactive phase could well be a minority species. Therefore, false photocurrent images should be treated as the stoichiometry required to form the photocatalytic phase under the experimental condition employed but not necessarily the stoichiometry of the photocatalytic phase.

The metal coverage (in units of mol/mm^2) is known for each element at each location on the ternary metal oxide thin film (Figure 1) because the drop volume, drop density, and

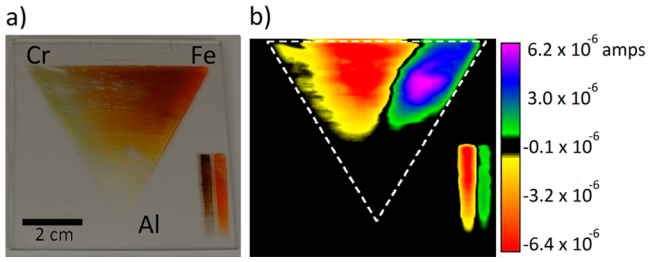

Figure 1. (a) Photograph of a ternary-gradient thin film metal oxide sample printed on a fluorine-doped tin oxide (FTO) substrate. Each vertex of the triangle pattern contains approximately the pure metal oxide phase of the following: Fe (upper right), Cr (upper left), and Al (bottom) oxide. The metal coverage (in mol/mm^2) changes across the triangle in a gradient such that at the metal coverage at the opposite edge of a vertex is approximately zero. Therefore, at each vertex, the metal oxide film is approximately pure single element, at the edges of the triangle the film is approximately a binary mixture of two elements, at any location within the triangle the film is a unique mixture of the three elements. The two strips at the bottom right are the p- and n-type internal standards of CuO and α-Fe_2O_3 respectively. (b) The false color photocurrent map of the ternary Fe, Cr, Al oxide thin film shown in panel a. The sample was immersed in 0.1 M NaOH aqueous electrolyte and scanned with a 532 nm laser under short circuit conditions in a two electrode configuration. The false color photocurrent map indicates that a p-type response is generated in the region that contains a mixture of iron, chromium, and aluminum. The CuO and α-Fe_2O_3 internal standards show the expected p- and n-type photocurrent, respectively. The white dashed triangle approximates the outline of the ternary-gradient metal oxide thin film.

precursor concentrations are known. Figure 1b shows the false color photocurrent map for the plate in Figure 1a that indicates an enhanced n-type photocurrent, in comparison with the internal standard α-Fe_2O_3, is generated region of the triangle-gradient pattern containing mostly binary mixtures of aluminum added to iron oxide. This result is in agreement with previous work that indicated that doping levels of ∼0.45 atomic percent of aluminum into α-Fe_2O_3 enhances the incident photon conversion efficiency (IPCE).[7,11] Interestingly, the enhanced photocurrent response of the aluminum-doped α-Fe_2O_3 region does not correspond to the region in the gradient pattern that matches the ideal atomic percentages reported in the literature, indicating that small amounts of chromium may also influence the photoactivity.[11]

The gradient pattern shown in Figure 1 is useful for surveying large regions of compositional space in the combinatorial discovery stage; however, producing and establishing the optimal stoichiometry of the photocatalyst requires a discrete printing pattern with regions of well determined metal amounts. If the composition of the metal oxide thin film changes on a smaller dimension than the interrogating laser spot size, then these smaller regions of high photocatalytic activity will show a relatively lower photocurrent due to averaging with the adjacent areas. The laser spot size, used to interrogate the photocatalytic activity of the metal oxide thin film samples, has a full width at half max of approximately 1 mm. Therefore, to more accurately determine the stoichiometry of the most photoactive region, a pattern with homogenous areas with small stoichiometry increments were printed that are much larger than the interrogating laser beam. The discrete printing template for printing the iron, chromium, and aluminum precursors is shown in Figure 2a.

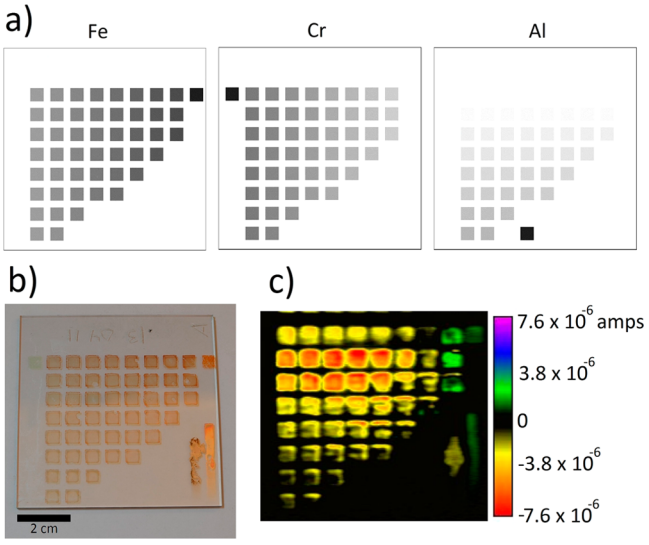

Figure 2. (a) Templates used to print the discrete ternary thin film metal oxide samples. This is an expanded discretized pattern of the most active p-type region shown in Figure 1. The squares represent regions where the 0.5 M metal nitrate salt ink solutions of iron, chromium, and aluminum were printed onto the FTO substrate. The opacity of the square is proportional to the number of 7 pL drops deposited per mm^2. The 7 pL drop density range was 335−670 drops/mm^2 for Fe, 86−207 drops/mm^2 for Cr, and 0−335 drops/mm^2 for Al. The two internal standard strips of CuO and α-Fe_2O_3 were also printed but are not depicted in these templates. (b) Photograph of the discrete ternary thin film metal oxide sample printed on fluorine-doped tin oxide (FTO) substrate. The atomic percentages (in mol/mm^2) for the three metals are homogenous for each square. The vertices of the triangular pattern are composed predominately of Fe (upper right), Cr (upper left), and Al (bottom) oxide. The metal coverage changes in regular increments between neighboring squares as shown in panel a. The two strips at the bottom right are the p- and n-type internal standards of CuO and α-Fe_2O_3, respectively. The film was printed with a spacing between drops of 30 μm. (c) False color photocurrent map of the ternary Fe, Cr, Al oxide thin film library shown in panel b. The sample was immersed in 0.1 M NaOH aqueous electrolyte and scanned with a 532 nm laser under short circuit conditions in a two electrode configuration. The false color photocurrent map indicates that a p-type response is generated in the region that corresponds to an oxide phase containing a mixture of iron, chromium, and aluminum with some iron rich regions showing n-type response. The CuO and α-Fe_2O_3 internal standards show the expected p- and n-type photoresponse.

Due to the variations between printed samples, the experiment in Figure 2 was repeated 6 times in order to calculate the average and the standard error for the determined optimal atomic percentages. Analysis using these discrete patterns reveals the optimal atomic fractions are 0.42 ± 0.03 parts iron, 0.50 ± 0.04 parts chromium, and 0.08 ± 0.02 parts aluminum for a phase stoichiometry of $Fe_{0.84}Cr_{1.0}Al_{0.16}O_3$ to achieve the highest photocurrent response under these experimental conditions.

Thin film X-ray diffraction (XRD) analysis confirms that the molar fractions determined above correspond to those in a crystalline photocatalytic phase (Figure 3). The cross section of the grazing incident X-ray beam used in the XRD acquisition is approximately 5 × 5 mm, much larger than the size of the 532 nm laser spot used to measure the false photocurrent maps. Therefore, XRD spectra could not be measured on the same sample used in Figure 2, but were instead measured on single composition metal oxide thin films that were printed across nearly the entire FTO substrate. Spinel structures of composition $Fe_{2-x-y}Cr_xAl_yO_3$ are well known;[12] however, XRD analysis indicates that the photoactive phase has a hexagonal structure similar to the elemental metal oxides. The lattice parameters for α-Fe_2O_3 and Cr_2O_3 are similar, whereas the unit cell of Al_2O_3 is substantially smaller. Additionally the atomic percentages of iron and chromium are required to form the photocatalytic phase are nearly identical. For these reasons, the iron and chromium atomic percentages were combined in Figure 3b, for the purposes of a Vegard's law analysis where the photocatalytic phase was represented with the formula $(Fe,Cr)_{2-x}Al_xO_3$. Vegard's law treatment of the FeCrAl oxide peak shift indicates that the atomic percentage for aluminum agrees with the atomic ratios of the metal nitrate salt precursors with all the aluminum incorporated into the crystalline phase. The lattice parameters (Table 1) used were calculated from the thin film diffraction patterns in Figure 3a. The thin film XRD data also shows contributions from the underlying FTO substrate. The extent of tin doping/migration in the FeAlCr oxide thin film is not known nor is the role of the FTO substrate as a template for forming the hexagonal rather than spinel phases.[11,13,14] This solid solution metal oxide phase of iron, chromium, and aluminum is, to our knowledge, previously unknown as a photoelectrolysis material.

The existence of binary phase diagrams for each permutation of the three elements suggests a three component solid solution is probable. The atomic percentages of the photocatalytic phase

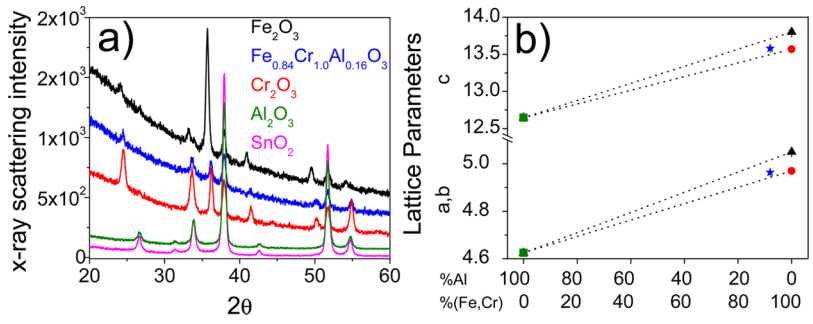

Figure 3. (a) Thin film X-ray diffraction (XRD) patterns for printed metal oxide thin films of Fe_2O_3 (back), $Fe_{0.84}Cr_{1.0}Al_{0.16}O_3$ (blue), Cr_2O_3 (red), and Al_2O_3 (green) on fluorine-doped tin oxide (magenta) substrate. (b) Plot of the lattice parameters for the metal oxide thin films calculated from the XRD spectra as a function of elemental composition. The crystal structure of the Fe_2O_3, Cr_2O_3, and Al_2O_3 are all hexagonal lattices with lattice parameters a, b, and c. The lattice parameters for the pure elemental metal phases Fe_2O_3 (black triangles), Cr_2O_3 (red circles), and Al_2O_3 (green squares) are shown. The lattice parameter and the aluminum atomic percentage of the photocatalytic phase are shown (blue star).

dx.doi.org/10.1021/am406045j | ACS Appl. Mater. Interfaces 2014, 6, 9046−9052

Table 1

phase	lattice parameters (a/b and c)
α-Fe_2O_3	5.05(3), 13.8(3)
Cr_2O_3	4.970(6), 13.57(2)
Al_2O_3	4.625, 12.645[a]
$Fe_{0.84}Cr_{1.0}Al_{0.16}O_3$	4.964(18), 13.58(5)

[a]XRD patterns for the Al_2O_3 film on FTO showed very little X-ray scattering from the Al_2O_3 film due to the low X-ray scattering efficiency of aluminum. The data base lattice parameters for Al_2O_3 were used for the Vegard's law analysis.[15]

reported here have been optimized for both light absorption and catalytic activity in the experimental conditions used. If the FeCrAl oxide system is a three component solid solution, then it should be possible to smoothly vary the composition along with the electronic and optical properties.

Scanning electron microscope (SEM) morphology images show small crystallites in the $Fe_{0.84}Cr_{1.0}Al_{0.16}O_3$ thin films. Cross section and surface images show dense thin films with a low surface roughness, Figure 4.

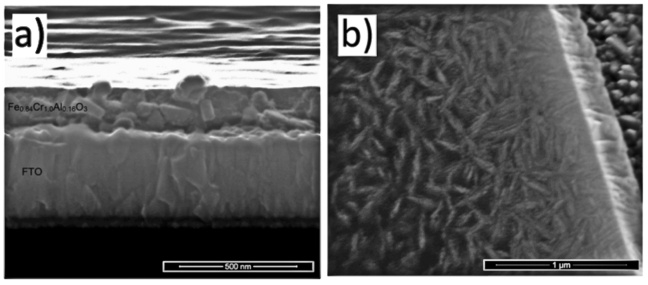

Figure 4. Scanning electron microscope (SEM) images of a $Fe_{0.84}Cr_{1.0}Al_{0.16}O_3$ film on a FTO substrate. The cross section (a) and top down (b) image of film both show small crystallites in the thin film. In panel a, the FTO substrate is approximately 450 nm thick. In panel b, the right hand side of the image is a crack in the film exposing the underlying FTO substrate.

Current–potential curves for the $Fe_{0.84}Cr_{1.0}Al_{0.16}O_3$ oxide thin film on an FTO substrate were measured in H_2(g) saturated 0.1 M perchloric acid aqueous electrolyte, an electrolyte composition that is different from the electrolyte used to measure the false photocurrent images in Figures 1 and 2. The electrolyte composition was changed for the IV measurements to insure that the observed p-type photoresponse was solely due to proton reduction and not due to the reduction of dissolved molecular oxygen.

The $Fe_{0.84}Cr_{1.0}Al_{0.16}O_3$ thin film shows a p-type photocurrent when illuminated as shown in Figure 5a. The 0.1 M perchloric acid aqueous electrolyte was de-oxygenated under an argon stream and then saturated by continually bubbling H_2 gas to provide a well-defined proton reduction potential during IV measurements.[8] The $Fe_{0.84}Cr_{1.0}Al_{0.16}O_3$ electrode shows a promising open circuit photovoltage that is almost a volt positive of the thermodynamic proton reduction potential in this electrolyte. The well-studied metal oxide semiconductor, n-type α-Fe_2O_3, has shown photovoltages of 0.5 V or less for oxygen evolution at current densities of 3 to 4 mA cm^{-2}.[20] The open circuit photovoltage of the $Fe_{0.84}Cr_{1.0}Al_{0.16}O_3$ electrode is impressive compared to that of α-Fe_2O_3 considering that the band gap of α-Fe_2O_3 is 2.2 eV, at least 1.6 volts of photovoltage would be needed for a single photoelectrode water splitting device or about 1.0 V for a tandem system. The fill factor and current density measured for this $Fe_{0.84}Cr_{1.0}Al_{0.16}O_3$ electrode have not been fully optimized through nanostructuring or high quality film fabrication techniques or deposition of hydrogen evolution catalysts on its surface. The optimization of the $Fe_{0.84}Cr_{1.0}Al_{0.16}O_3$ photocatalytic phase will be the subject of future investigations.

Figure 5b shows a chronoamperometric photocurrent plot at 0.46 V vs NHE for the $Fe_{0.84}Cr_{1.0}Al_{0.16}O_3$ thin film on FTO in the same H_2(g) saturated 0.1 M perchloric acid aqueous electrolyte. The photocurrent response to the 70 s light pulse indicates that significant charge recombination is occurring in this material at this potential.[16] The photocurrent is certainly reduced by the absence of a hydrogen evolution catalyst on the surface that would be required for high steady state proton reduction photocurrents. Longer chronoamperometric measurements indicate that the photocurrent does eventually reach a steady state value of 5% of the initial current density spike over the course of 30 min. The cause of this decrease in photocurrent is unknown but may be due to film delamination because the decrease in photocurrent does not fully recover in the dark.[6] Previous work on p-type oxides for hydrogen reduction revealed that extended illumination at negative applied potentials reduces the FTO film that results in

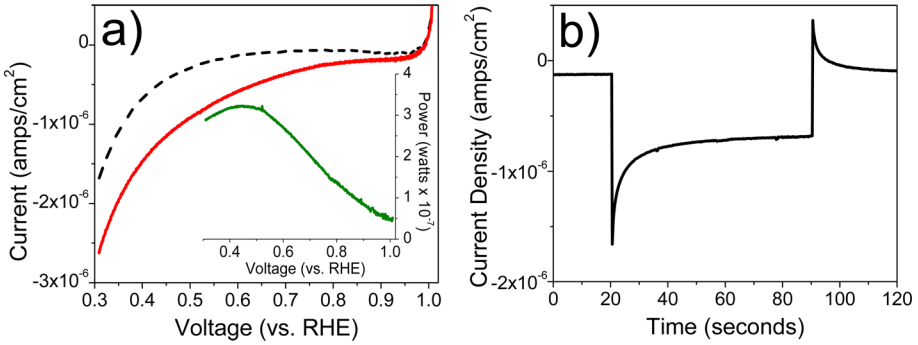

Figure 5. (a) Current–potential curves and power curve (inset) for a $Fe_{0.84}Cr_{1.0}Al_{0.16}O_3$ thin film on an FTO substrate in the dark (black dashed) and continuously illuminated with 532 nm laser light (red). The inset shows the power curve, the product of the current and voltage. Current–potential curves were measured in H_2(g) saturated aqueous 0.1 M perchloric acid solution in a three electrode configuration. Back-side illumination was employed with a 532 nm laser light with a power density of 30 mW/cm^2. (b) Chronoamperometric measurement for the same $Fe_{0.84}Cr_{1.0}Al_{0.16}O_3$ thin film under the same conditions as in panel a. A bias of 0.46 V vs RHE was applied. Initially, the thin film was in the dark, then 20 s into the experiment, the sample was illuminated with the 532 nm laser. The illumination was stopped after 90 s.

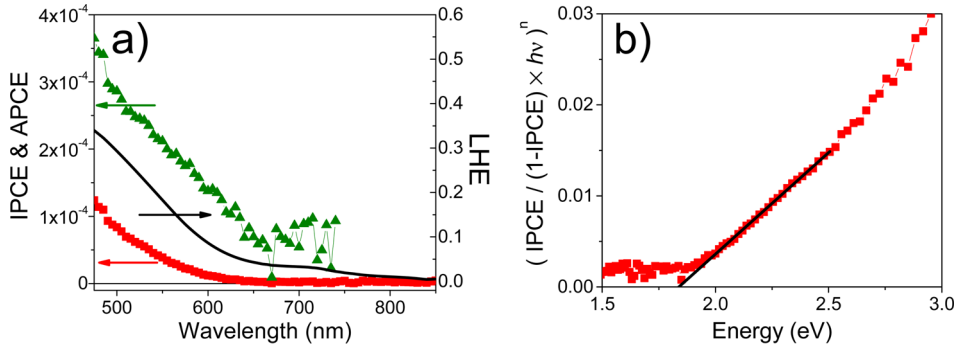

Figure 6. (a) Incident photon to current efficiency (IPCE) spectra (red squares), transmission mode UV−Vis 1 (absorptance or light harvesting efficiency (LHE) spectra (black line)), and absorbed photon to current efficiency (APCE) spectrum (green triangles) of a FeCrAl oxide on an FTO substrate immersed in $H_2(g)$ saturated aqueous pH 1 perchloric acid solution. The IPCE spectrum was measured in a three electrode configuration with an applied bias near the power point of the cell at approximately 0.6 V vs RHE. The approximately 1 cm^2 sample was illuminated with a lamp intensity of 5×10^{-6} W/cm^2 at 532 nm. (b) Tauc-type plot of the IPCE spectra in panel a where $n = 1/2$. Tauc plots using n values of 1 and 2 did not show linear regions.

delamination of the film and a similar process could be happening in this case.

The incident photon conversion efficiency (IPCE) spectra for the $Fe_{0.84}Cr_{1.0}Al_{0.16}O_3$ thin film on an FTO substrate was measured in $H_2(g)$ saturated 0.1 M perchloric acid aqueous electrolyte. The IPCE spectrum has nearly the same spectral shape as the transmission mode UV−Vis absorptance spectrum (LHE spectrum) of the film immersed in the same 0.1 M perchloric acid solution (Figure 6a).

Figure 6b shows a Tauc plot of the IPCE spectrum with $n = 1/2$. The data is highly linear above 2 eV, indicating that $Fe_{0.84}Cr_{1.0}Al_{0.16}O_3$ has an indirect band gap. Extrapolation of the linear region between 2 and 2.5 eV to the x-intercept indicates the band gap of the $Fe_{0.84}Cr_{1.0}Al_{0.16}O_3$ is about 1.8 eV (689 nm)[17] close to the ideal band gap for the top layer of a tandem photoelectrolysis device that is between 1.7 and 2.0 eV.[18,19] However, this ideal bandgap is calculated based on getting nearly ideal photovoltages from each material and the ∼1.0 V obtained is a good value for an initial study especially when no hydrogen evolution catalysts were deposited on the surface.

The IPCE at 530 nm in Figure 6 is 5.5×10^{-5}; this value is in close agreement with the IV curve data shown in Figure 4 where the sample is illuminated with a 30 mW of laser light that generates a photocurrent at the power point of approximately 3.7 μamps/cm^2. This would give an IPCE value of approximately 3×10^{-5}. In the absence of surface modification with a proton reduction catalysts and/or film nanostructuring, the absorbed photon to conversion efficiency (APCE) for the $Fe_{0.84}Cr_{1.0}Al_{0.16}O_3$ thin film serves as a benchmark for optimization of the material properties. The APCE is calculated from the IPCE and the light harvesting efficiency (LHE) using eqs 1 and 2

$$\text{APCE} = \text{IPCE}/\text{LHE} \quad (1)$$

$$\text{LHE} = 1 - 10^{-\text{abs}(\lambda)} \quad (2)$$

where $\text{Abs}(\lambda)$ is the FeCrAl oxide thin film absorbance value at a given wavelength. Taking the data shown in Figure 4, the IPCE and LHE values at 530 nm are 5.5×10^{-5} and 0.23, respectively. The APCE value for this sample was calculated to be 2.4×10^{-4} using eqs 1 and 2. These quite low values need to be improved perhaps by better coupling of the nanosized crystals to the each other and the substrate, changing the film morphology or by improving the rate of hydrogen evolution by depositing catalysts because surface recombination is a problem with poor hydrogen evolving surfaces expected on oxide materials. Further enhancements in overall absorption and IPCE values could be achieved via nanostructuring of the films, and will be the subject of future studies.[20]

The inkjet printing technique is intended for rapid discovery of promising semiconductor materials; the inkjet printing technique has not been designed for efficient device fabrication because the films are printed very thin and diffusion lengths of carriers in these materials is expected to be very small. The indirect transition also indicates that a thin film will absorb only a small fraction of incident light. Further investigations of FeCrAl oxides should concentrate on optimizing optical properties, electronic properties and co-catalyst composition and structure to produce more efficient hydrogen evolving photocathodes.

CONCLUSION

The Solar Hydrogen Research Activity Kit (SHArK) program has over 6 years of participation and fruitful learning and scientific discovery by young scientists. We have demonstrated that a combinatorial and distributed science outreach programs such as SHArK are capable of producing new science including the discovery of new semiconducting metal oxide photoelectrolysis catalysts.

A FeCrAl oxide, with previously unreported p-type photoelectrolysis properties, was discovered by a young undergraduate scientist (Thanh D. Do) participating in the SHArK program. The identity and some of the photoelectrolysis properties of this FeCrAl oxide were determined including an optimal and likely a solid solution stoichiometry of around $Fe_{0.84}Cr_{1.0}Al_{0.16}O_{3b}$ with the α-Fe_2O_3 structure suggesting the ability to further optimize the composition of the photoactive phase. The photocurrent spectrum of the $Fe_{0.84}Cr_{1.0}Al_{0.16}O_3$ photoelectrode has an onset near 689 nm or 1.8 eV, which makes it a promising candidate as the p-type layer in a tandem cell. The open circuit photovoltage of a $Fe_{0.84}Cr_{1.0}Al_{0.16}O_3$ thin film photoelectrode for hydrogen evolution was nearly 1.0 V. The baseline APCE was calculated to be 2.4×10^{-4} at 530 nm. Nanostructuring and high quality metal oxide film synthesis techniques plus deposition of hydrogen evolution catalysts are expected to greatly improve the APCE for this material. SEM images and XRD spectra indicate nanosized crystallites of a

dx.doi.org/10.1021/am406045j | ACS Appl. Mater. Interfaces 2014, 6, 9046−9052

hexagonal crystalline phase of the earth abundant $Fe_{0.84}Cr_{1.0}Al_{0.16}O_3$ semiconductor. These properties make an FeCrAl oxide a promising candidate for further study and perhaps eventual application in a photoelectrolysis device.

■ ASSOCIATED CONTENT

Supporting Information

False photo current image and experimental details from Gonzaga University SHArK participants indicating a promising photoelectrolysis material had been discovered that contained some ternary combination of the following elements: iron, chromium, aluminum, and cesium and a schematic of the scanning laser system used for producing the false photocurrent images. This material is available free of charge via the Internet at http://pubs.acs.org.

■ AUTHOR INFORMATION

Corresponding Author

*B. A. Parkinson. E-mail: bparkin1@uwyo.edu.

Present Addresses

[†]Department of Chemistry, Carroll College, Helena, MT 59625
[‡]Department of Chemistry & Biochemistry, Gonzaga University, Spokane, WA 99258
[§]Department of Chemistry & Biochemistry, University of California, Santa Barbara, CA 93106-9510

Notes

The authors declare no competing financial interest.

■ ACKNOWLEDGMENTS

The authors recognize the determination and creativity of the many high school and undergraduate students who have participated in the SHArK project over the last 6 years. In addition, we thank the research mentors at the participating high school and undergraduate institutions who facilitate the implementation of the SHArK distributed research program. This work was funded by the Division of Chemical Sciences, Geosciences, and Biosciences, Office of Basic Energy Sciences of the U.S. Department of Energy through Grant #DE-FG02-05ER15750. The SHArK project was initially funded by a Dreyfus Grant and has recently been supported by the NSF Funded Center for Chemical Innovation entitled Powering the Planet under Grant #CHE-0802907.

■ REFERENCES

(1) Hermann, W. A. Quantifying Global Energy Resources. *Energy* **2006**, *31*, 1685−1702.
(2) Lewis, N. S.; Nocera, D. G. Powering the Planet: Chemical Challenges in Solar Energy Utilization. *Proc. Natl. Acad. Sci. U. S. A.* **2006**, *103*, 15729−15735.
(3) Woodhouse, M.; Parkinson, B. A. Combinatorial Approaches for the Identification and Optimization of Oxide Semiconductors for Efficient Solar Photoelectrolysis. *Chem. Soc. Rev.* **2009**, *38*, 197−210.
(4) Gregoire, J. M.; Xiang, C.; Mitrovic, S.; Liu, X.; Marcin, M.; Cornell, E. W.; Fan, J.; Jina, J. Combined Catalysis and Optical Screening for High Throughput Discovery of Solar Fuels Catalysts. *J. Electrochem. Soc.* **2013**, *160*, F337−F342.
(5) Anunson, P. N.; Winkler, G. R.; Winkler, J. R.; Parkinson, B. A.; Schuttlefield, J. D. Involving Students in a Collaborative Project to Help Discover Inexpensive, Stable Materials for Solar Photoelectrolysis. *J. Chem. Educ.* **2013**, *90*, 1333−1340.
(6) Woodhouse, M.; Parkinson, B. A. Combinatorial Discovery and Optimization of a Complex Oxide with Water Photoelectrolysis Activity. *Chem. Mater.* **2008**, *20*, 2495−2502.
(7) He, J. H.; Parkinson, B. A. Combinatorial Investigation of the Effects of the Incorporation of Ti, Si, and Al on the Performance of alpha-Fe(2)O(3) Photoanodes. *ACS Comb. Sci.* **2011**, *13*, 399−404.
(8) Walter, M. G.; Warren, E. L.; McKone, J. R.; Boettcher, S. W.; Mi, Q. X.; Santori, E. A.; Lewis, N. S. Solar Water Splitting Cells. *Chem. Rev.* **2010**, *110*, 6446−6473.
(9) Parkinson, B. A. Distributed Research: A New Paradigm for Undergraduate Research and Global Problem Solving. *Energy Environ. Sci.* **2010**, *3*, 509−511.
(10) Parkinson, B. A. The Solar Hydrogen Research Kit Project. *SPIE Newsroom* [Online] **2013**, DOI: 10.1117/2.1201110.003814. http://spie.org/documents/Newsroom/Imported/003814/003814_10.pdf (accessed July 31, 2013).
(11) Shwarsctein, A. K.; Huda, M. N.; Walsh, A.; Yan, Y.; Stucky, G. D.; Hu, Y.; Al-Jassim, M. M.; McFarland, E. W. Electrodeposited Aluminum-Doped α-Fe_2O_3 Photoelectrodes: Experiment and Theory. *Chem. Mater.* **2010**, *22*, 510−517.
(12) Qasim Jan, M.; Asif Khan, M.; Windley, B. F. Exsolution in Al-Cr-Fe^{3+}-rich Spinels from the Chilas Mafic-Ultramafic Complex, Pakistan. *Am. Mineral.* **1992**, *77*, 1074−1079.
(13) Ramm1, J.; Ante1, M.; Brändle1, H.; Neels, A.; Dommann, A.; Döbeli, M. Thermal Stability of Thin Film Corundum-Type Solid Solutions of $(Al_{1-x}Cr_x)_2O_3$ Synthesized Under Low-Temperature Non-Equilibrium Conditions. *Adv. Eng. Mater.* **2007**, *9*, 604−608.
(14) Kleiman-Shwarsctein, A.; Hu, Y.; Forman, A. J.; Stucky, G. D.; McFarland, E. W. Electrodeposition of α-Fe2O3 Doped with Mo or Cr as Photoanodes for Photocatalytic Water Splitting. *J. Phys. Chem. C* **2008**, *112*, 15900−15907.
(15) Kim-Zajonz, J.; Werner, S.; Schulz, H. High Pressure Single Crystal X-ray Diffraction Study on Ruby up to 31 GPa. *Z. Kristallogr.* **1999**, *214*, 331−336.
(16) Peter, L. M. Dynamic Aspects of Semiconductor Photoelectrochemistry. *Chem. Rev.* **1990**, *90*, 753−769.
(17) Kam, K. K.; Parkinson, B. A. Detailed Photocurrent Spectroscopy of the Semiconducting Group VI Transition Metal Dichalcogenides. *J. Phys. Chem.* **1982**, *86*, 463−467.
(18) Bolton, J. R.; Strickler, S. J.; Connolly, J. S. Limiting and Realizable Efficiencies of Solar Photolysis of Water. *Nature* **1985**, *316*, 495−500.
(19) Weber, M. F.; Dignam, M. J. Splitting Water with Semiconducting Photoelectrodes − Efficiency Considerations. *Int. J. Hydrogen Energy* **1986**, *11*, 225−232.
(20) Kay, A.; Cesar, I.; Grätzel, G. New Benchmark for Water Photooxidation by Nanostructured α-Fe_2O_3 Films. *J. Am. Chem. Soc.* **2006**, *128*, 15714−15721.